RADIANT–CONVECTIVE HEAT EXCHANGE IN FLOW OF A HIGH-TEMPERATURE GAS SUSPENSION OVER A SURFACE

V. E. Abaltusov and N. N. Ponomarev

UDC 536.25:536.542

Results are offered from experimental and theoretical studies of complex heat exchange in flow of a high-temperature dusty stream over a plane plate.

Studies of heat exchange on a surface over which there flows an absorbing, radiating, and scattering medium are of great importance in the study of the thermal state of various industrial equipment used in high-temperature technology [1-6]. At present the factors determining heat–mass exchange in such media have not been studied sufficiently. Calculation of gas flows with suspended particles is quite complicated, since aside from the fact that the character of particle interactions among themselves and with the gas is often unknown, it is necessary to consider the radiation of the two-phase flows. Experimental measurement methods developed for study of high temperature gas flows are not always suitable for determining parameters of radiant–convective heat exchange in dusty flows, while on the other hand, methods used for study of dusty gas flows at moderate temperature do not permit determination of heat-exchange parameters at high temperature.

The present study will offer results of combined experimental and theoretical studies of complex heat exchange in flow of a high-temperature dusty flow over a plane plate. The experimental studies were performed with equipment including a gas dynamic testing system based on an electric arc plasmotron, a measurement-computation complex containing measurement units for stream parameters, heat–mass exchange characteristics, and optical diagnostics [5].

The fundamental parameters of the high-temperature two-phase flow are the temperature of the gas T_e and particles T_p, the velocity of gas U_e and particles U_p, and the concentrations of the gaseous and solid components. Methods for measurement of two-phase flow parameters were presented in [5, 7]. Measurements of the gas temperature distribution along the axis of symmetry of the plasma jet were performed by optical and contact methods. Each of these methods is usable over a certain temperature range. In the stream segment $\bar{x} > 6$ (where $\bar{x} = x/d$, x being the distance from the nozzle section along the jet axis; d, the diameter of the plasmotron nozzle) a thermoelectric method of temperature measurement was used, with PP-1 thermocouples. Near the nozzle section at distances $\bar{x} \leq 6$ temperature measurement was performed by a spectral method (see Fig. 1, II). To record the energy distribution in the spectrum a KSVU-223 universal spectral device based on an MDR-23 monochromator was used. The temperature was determined using relative intensities of nitrogen and copper lines, it being assumed that the gas state in the plasma jet at atmospheric pressure was close to equilibrium [7]. To estimate temperature nonequilibrium of the particles the brightness temperature of a set of particles was measured. The true particle temperature T_p was defined for particles of materials with known emissivities in the wavelength range $\lambda = 0.65 \pm 0.007$ μm. The particle velocity was found using an ISSO-1 bright object velocity meter [7]. The measurement technique is based on comparing the velocities of the test and reference object by a time display of the image of the object perpendicular to its direction of motion (Fig. 1, I). Figure 2 shows phase temperature and velocity distributions of the two-phase plasma jet.

In the experiments submerged jet flow was realized, the jet being bounded on one side by a solid plane wall upon which a boundary layer is formed [8]; the gas flow parameters on the leading edge of the plate were: H_e = 3-6 MJ/kg, $M \leq 0.4$, $Re = 10^3$-10^4. Particles of Al, Al_2O_3, or graphite were used for the suspended phase; particle mass concentration was κ = 0-0.7.

Applied Mathematics and Mechanics Scientific-Research Institute at Tomsk State University. Translated from Inzhenerno-Fizicheskii Zhurnal, Vol. 56, No. 5, pp. 749-753, May, 1989. Original article submitted April 19, 1988.

 0022-0841/89/5605-0528$12.50

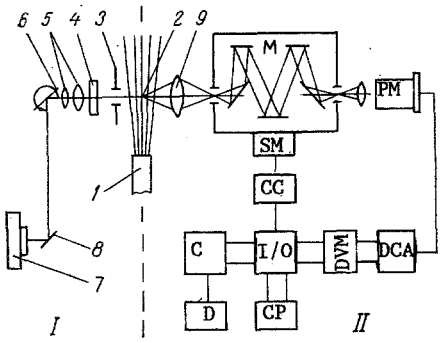

Fig. 1

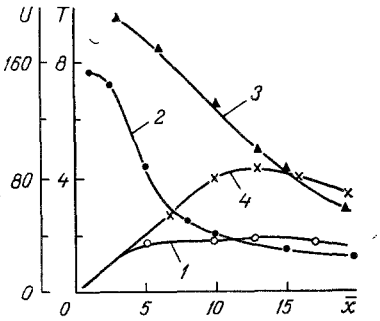

Fig. 2

Fig. 1. Gas and particle temperature and velocity measurement system: 1) plasmotron nozzle; 2) particle trajectory; 3) diaphragm; 4) light filter; 5) objective lens; 6) mirror; 7) camera; 8) rotating mirror; 9) lens; M) MDR-23 monochromator; SM) stepper motor; CC) control circuit; C) calculator; D) display; CP) control panel; DVM) digital voltmeter; DCA) dc amplifier; I/O) input/output device.

Fig. 2. Particle and gas temperature and velocity measurements: 1) graphite particle temperature; 2) gas temperature; 3) gas velocity; 4) particle velocity. U, m/sec; T, 10^3 K.

The distribution of local thermal flux along the plate was measured and the flow pattern studied. To measure the total thermal flux to the surface flowed over, transient colorimeters with thermocouple recording were used, installed at five points along the plate [5]. The heat balance on the surface of a sensitive element of thickness δ can be written in the form

$$q_w(t)=q_0(t)+q_1(t)+q_2(t), \qquad (1)$$

where $q_0 = \rho c_p \delta dT/dt$; q_1 is heat leakage into the insulator, $q_2 = \varepsilon\sigma T_w^4$ is the radiant thermal flux from the sensitive element surface.

Calculation of thermal fluxes and measurement uncertainties was performed by the method of [7] using the VOLT program with a minicomputer-based automated complex.

To distinguish the radiant component from the total heat flux, special sensors were used with the sensitive element located within the body with the radiant thermal flux first passing through a special window of material transparent to the incident radiation.

The sensor element used was a copper calorimeter with blackened surface, the temperature of which was measured by an Ch–Al thermocouple. The thermal fluxes q_r were calculated by a method similar to the total flux calculation. The total and radiant thermal fluxes were also calculated by the method of [9] by solving the converse thermal conductivity problem. The thermal flux was determined by solving the nonlinear thermal conductivity equation for the temperature measured at the boundary of the sensitive element and insulator. Comparison of the solutions of the converse problem obtained by the method of [9] and with Eq. (1) showed that they differed insignificantly at low sensitive element thickness values ($\delta \approx 1$ mm) and low temperatures, which is apparently the result of practically complete temperature equalization in the sensitive element. At high sensitive element temperatures ($T > 500$ K) the effect of change in the thermophysical properties of the sensitive element and insulator materials becomes significant.

Figure 3 shows the dependence of the ratio of radiant thermal flux q_r to the total flux q_Σ upon longitudinal coordinate $\bar{\xi}$. Near the leading edge of the plate ($\bar{\xi} \to 0$) the effect of the radiation on convective heat exchange is insignificant, with increase in the optical parameter $\bar{\xi}$ there is a growth in the radiant component of the thermal flux. It was also noted that at $\bar{\xi} \geq 0.6$ the interaction of convection and radiation intensifies heat exchange and the fraction of radiation then depends only weakly on the material composition of the particle.

In contrast to the gray medium approximation, the calculations of radiant thermal fluxes in the dispersed medium were carried out by a complex method including determination of the radiant properties of an elementary volume of the medium and calculating spectral and integral

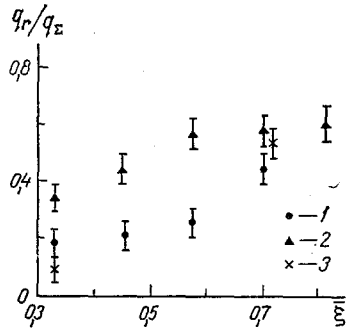

Fig. 3

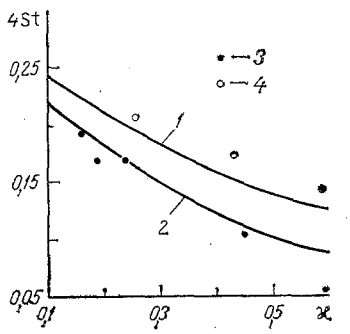

Fig. 4

Fig. 3. Ratio of radiant thermal flux to total flux vs longitudinal coordinate: 1) air–graphite, $d_p \leq 100$ μm, $\kappa = 0.08$-0.15; 2) air–Al, $d_p \leq 50$ μm, $\kappa = 0.08$-0.2; 3) air–Al_2O_3, $d_p \leq 50$ μm, $\kappa = 0.18$-0.3.

Fig. 4. Comparison of experimental and calculated data: 1, 4) Al_2O_3; 2, 3) graphite (curves, experiment; points, experiment).

characteristics of the radiation field. To find the radiant characteristics of the medium an algorithm based on MI theory was used, the monochromatic transport equation was solved by a modified SP-method. The dusty medium was modeled by a monodispersed system consisting of spherical particles of graphite and aluminum oxide. To obtain more complete information on optical constants theoretical studies were performed, including solution of the converse problem and comparative analysis of the data of various authors, the converse problem was realized by the probe method. In the theoretical study steady-state laminar flow over a plane plate by a high-temperature gas suspension with selective radiation spectrum was considered [4]. The dusty flow was considered to be a gas with effective values of density $\bar{\rho} = \rho(1 + \kappa)$, specific heat $\bar{c}_p = c_p(1 + \kappa\bar{c})/(1 + \kappa)$, and kinematic viscosity $\bar{\nu} = \nu/(1 + \kappa)$. The formulation of the problem reduces to a system of boundary-layer equations. The energy equation and boundary conditions are written in the following dimensionless form:

$$\bar{\xi} f' \frac{\partial\theta}{\partial\bar{\xi}} = \frac{1}{\mathrm{Pr}} \frac{\partial^2\theta}{\partial\bar{\eta}^2} + \frac{1}{2} f \frac{\partial\theta}{\partial\bar{\eta}} - \frac{\bar{\xi}}{\bar{B}_0} \int_0^\infty \{\bar{h}_{0\lambda}(1+\omega_\lambda)[4\pi\bar{B}_{0\lambda}(\theta) -$$

$$-\Phi_{*\lambda}(h_\lambda)]\}\, d\lambda; \quad \theta = \theta_0(\bar{\eta}),\ \bar{\xi} = 0;\ \theta = \theta_w,\ \bar{\eta} = 0;\ \theta \to \theta_\infty,\ \bar{\eta} \to \infty.$$

The similarity parameters of the problem have the form $\bar{\mathrm{Pr}} = \mathrm{Pr}\ (1 + \kappa\bar{c})/(1 + \kappa)$, $\bar{B}_0 = B_0(1 + \kappa\bar{c})$, $\bar{\mathrm{Re}}_L = \mathrm{Re}_L(1 + \kappa)$, where the values of Pr, B_0, Re_L correspond to the flow of a pure gas ($\kappa = 0$).

To study local heat liberation, the Stanton criterion was introduced in the form $\mathrm{St} = q_w/[4\bar{B}_0(\theta_w - 1)]$. The temperature field calculations performed indicate an increase in the physical thickness of the thermal boundary layer as compared to calculations in the gray medium approximation.

The experimental and calculated data were compared for the following parameter values: $T_e \approx 2000$ K, $T_w \approx 950$ K, $U_e = 50$-200 m/sec.

The carrier medium used for the two-phase flow was air, with mass concentration of aluminum oxide and graphite particles varied over the range $\kappa = 0.1$-0.7. Figure 4 shows some results of comparing experimental and calculated data in the form of the dependence of the net Stanton number St on mass concentration of solid phase particles. It is evident that with increase in particle concentration St decreases markedly. It was found that in the region of large particle size the Stanton number depends weakly on material composition and size of the dispersed phase, but is determined by the particle mass concentration level in the layer.

NOTATION

κ, relative particle mass concentration; $\bar{c}$, ratio of particle specific heat to gas specific heat; $\bar{\xi} = x/L$, dimensionless longitudinal coordinate; L, plate length; $\mathrm{Re}_L = U_e L/\nu$,

Reynolds number; $\theta = T/T_e$, temperature; $f(\eta)$, Blasius function; η, self-similar variable; $h = ky$, optical depth of layer; h_0, optical thickness of layer; ω, single-scattering albedo; $h_\lambda = h_{0\lambda}(\bar{\xi}/\mathrm{Re}_L)^{1/2}\eta$, optical depth of boundary layer; $\bar{h}_{0\lambda} = k_\lambda L$, longitudinal optical thickness of layer; $\bar{B}_{0\lambda} = B_{0\lambda}/4\sigma T_e^4$; $B_{0\lambda}$, spectral intensity of ideal black body radiation; $\Phi_{*\lambda} = J_\lambda/4\sigma T_e^4$, dimensionless flux density of incident volume radiation; H, enthalpy; q, thermal flux; ρ, c_p, density and specific heat of calorimeter material; ε, integral emissivity of wall material; σ, Stefan–Boltzmann constant. Subscripts: e, parameters at external boundary of boundary layer; w, wall; λ, spectral.

LITERATURE CITED

1. N. N. Ponomarev and N. A. Rubtsov, Izv. Akad. Nauk SSSR, Ser. Tekh. Nauk, No. 13, 98-103 (1980).
2. L. T. Grebeshnikov, É. A. Zverev, V. Ya. Klabukov, et al., Radiant Heat Exchange in Technology [in Russian], Kaunas (1987), pp. 39-40.
3. L. A. Dombrovskii and L. G. Barkova, Teplofiz. Vys. Temp., 24, No. 4, 762-769 (1986).
4. N. N. Ponomarev and N. A. Rubtsov, Heat-Mass Exchange [in Russian], Vol. 2, Minsk (1984), pp. 20-24.
5. V. E. Abaltusov, Heat-Mass Exchange in Thermal Protection Systems with Active Mass Draft [in Russian], Dep. VINITI, No. 535-85, Jan. 21, 1985.
6. Yu. V. Polezhaev and F. B. Yurevich, Thermal Protection [in Russian], Moscow (1976).
7. V. E. Abaltusov, N. N. Alekseenko, V. F. Dement'ev, et al., Gagarin Scientific Studies on Cosmonautics and Aviation [in Russian], Moscow (1987), pp. 158-159.
8. É. P. Volchkov, Gas Suspensions on Walls [in Russian], Novosibirsk (1983).
9. V. E. Abaltusov, S. F. Bachurina, G. Ya. Mamontov, et al., Inzh.-Fiz. Zh., 49, No. 5, 763-769 (1985).

SPATIAL AND POLARIZATION CHARACTERISTICS OF RADIATION REFLECTED BY COMPOSITE MATERIALS

E. A. Garnova, Ya. M. Geda, V. A. Dlugunovich, and V. N. Snopko

UDC 535.312

In the spectral regions 0.63 and 1.15 μm, measurements are made of the degree of polarization and indicatrix of radiation reflected from the surface of composite materials before and after their heating in air by radiation from a CO_2 laser.

Increasing use is being made of composite materials in different areas of modern technology, the annual output of these materials now accounting for ~25% of production [1]. In a number of cases, lasers turn out to be the most appropriate tool for processing composites under industrial conditions. Here, one of the main parameters which characterizes the efficiency of energy expenditure in laser processing is the reflection coefficient [2, 3].

Detailed study of processes involved in the interaction of laser radiation with materials requires information not only on the reflection coefficient, but also on the polarization and spatial characteristics of the reflected radiation. This information is necessary in measuring the thermodynamic temperature by optical methods [4], in developing measurement systems to study the reflection coefficients and temperature of materials, and in calculating radiative heat transfer by high-temperature structures [5].

In the present study, at wavelengths of 0.63 and 1.15 μm, we measured the degree of polarization and indicatrix of radiation reflected from the surfaces of glass-textolite STK,

Institute of Physics, Academy of Sciences of the Belorussian SSR, Minsk.

Translated from Inzhenerno-Fizicheskii Zhurnal, Vol. 56, No. 5, pp. 753-759, May, 1989. Original article submitted November 18, 1987.